Determination of oxidized metals' oxide layer thickness from local extrema of reflectance spectra: theoretical basis and application to anodized titanium

Renée Charrière, Quentin Cridling, Maxence Maillet, Mariapia Pedeferri, David Delafosse

Determination of oxidized metals' oxide layer thickness from local extrema of reflectance spectra: theoretical basis and application to anodized titanium

Renée Charrière[1], Quentin Cridling[1,2]‡, Maxence Maillet[1], MariaPia Pedeferri[2], David Delafosse[1,2]

[1]Mines Saint-Etienne, Univ Lyon, CNRS, UMR 5307 LGF, Centre SMS, F - 42023 Saint-Etienne France

[2]Politecnico di Milano, Department of Chemistry, Materials and Chemical Engineering "Giulio Natta", Milan, Italy

E-mail: renee.charriere@emse.fr

Abstract. The present paper concerns the oxide layer thickness determination of oxidized metals in the case where an optical interference phenomenon occurs inside the oxide layer. The paper focuses on anodized titanium. It establishes theoretical formula to compute the oxide layer thickness from the local extrema positions of the material reflectance spectra. These formula take into account the air/oxide and oxide/metal interfaces electromagnetic phase-shift and are valid for TE, TM and non-polarized light, and for all incidence angles. By applying these formula to simulated reflectance spectra with known oxide thicknesses, it shows that neglecting the interfaces phase-shift is inappropriate to determine the oxide thickness of samples with thin oxide thicknesses. When the interfaces phase-shift is taken into account, a careful attention needs to be paid to the light polarization for incidence angles close to the Brewster angle of the air/oxide interface. The relative error on the oxide thickness determination is relatively good correlated to the relative standard deviation characterizing the discrepancy of the oxide thickness values obtained from different extrema positions. The typical behavior with polarization and incidence angle of this standard deviation predicted by the theoretical study is in agreement with the behavior observed for titanium samples.

Keywords: anodized titanium, oxide thickness determination, interference phenomenon, reflectance spectrum, local extrema

‡ Present address: Laboratoire Commun de Métrologie, LNE-CNAM, 93210 La Plaine-Saint-Denis, France

1. Introduction

Under certain conditions, when an oxide layer grows on the top of a metal, an interference phenomenon can occur inside the oxide layer. This is the case for example for titanium, aluminum, cobalt, zirconium, tantalum and niobium [1, 2, 3, 4, 5, 6, 7]. In this case, the material reflectance spectrum exhibits minima and maxima which positions can be linked to the oxide layer thickness.

Even though this method is widely used for oxide thickness determination, very few papers take into account the electromagnetic phase-shift which occurs at the reflection on the air/oxide and oxide/metal interfaces when establishing the formula linking the positions of the local extrema to the oxide thickness. References [8, 9, 10, 11, 12, 13, 1, 14, 15] neglect this phase-shift, whereas Fuhrman et al. [16] mention it but don't give a detailed calculation of its theoretical value. Charlesby et al. [17] characterized anodized tantalum samples by taking into account the electromagnetic phase-shift. They developed an original method to determine experimentally at the same time the variations of the oxide refractive index with the wavelength, the oxide layer thickness, and the evolution with wavelength of the oxide/metal electromagnetic phase-shift. Winterbottom [18] gave theoretical relationships between the reflectance spectra local extrema positions and the oxide layer thickness taking into account the oxide/metal electromagnetic phase-shift. He also compared oxide thickness values estimated with and without taking into account the oxide/metal electromagnetic phase-shift for various oxide/metal systems (Cu_2O/Cu, Fe_2O_3/Fe, Al_2O_3/Al) and showed that the thickness estimation error can reach about 200% when the phase-shift is neglected. Pliskin [19] established theoretical formulas of the electromagnetic phase-shift for Transverse Electric (TE) and Transverse Magnetic (TM) electric field polarizations and computed phase-shift thickness correction charts for various systems as for example silicon dioxide (SiO_2)/Aluminum, SiO_2/Chromium, Alumina/Germanium... with the refractive indexes of the different materials extracted from the literature. For example, if the reflectance measurement is done at an incidence angle of 60° on an SiO_2/Silver system, the thickness correction can reach 39 nm for TE polarization and 64 nm for TM polarization. Note that Charlesby et al. [17] don't take into account a possible influence of the light polarization on the electromagnetic phase-shift. Also, the theoretical formulas given by Winterbottom [18] are valid for normally incident light where TE and TM polarized light cannot be distinguished.

The present paper focuses on anodized titanium, that is titanium on which an oxide layer has been made grown through an electrochemical process. The paper establishes formulas giving the oxide thickness from the reflectance spectra maxima and minima positions for TE, TM and non-polarized light, for all incidence angles. These formula take into account the interfaces electromagnetic phase-shift. The validity of these formulas is then checked and discussed by applying them to simulated reflectance spectra with known oxide thicknesses. The error on the oxide thickness made when neglecting the interfaces electromagnetic phase-shift is also presented. To check if the conclusions deduced from the simulated spectra are suitable for experimental data, the formula are applied to reflectance spectra measured on anodized titanium samples.

2. Theoretical basis for the calculation of the oxide layer thickness from reflectance spectra local extrema

This section will recall the theoretical background of the interference phenomenon occurring inside the oxide layer. It will then establish the formulas giving the oxide thickness from the reflectance maxima and minima positions. The material is here assumed as a perfectly flat and homogeneous layer of titanium dioxide (TiO_2) with a refractive index n_{TiO_2} on top of a semi-infinite perfectly flat and homogenous titanium (Ti) substrate with a refractive index n_{Ti}. The model presented in this section assumes that the TiO_2 layer is non-absorbent: n_{TiO_2} is thus supposed to have a null imaginary part. In the wavelength range [370 nm 800 nm] considered here, anodically grown titanium dioxide indeed has a refractive index imaginary part lower than 0.5 [20, 21]. The interference phenomenon occurring in anodized titanium is described in figure 1. An electric field is incident on the sample surface with a wave-vector (propagation direction) $\vec{k}_0$ corresponding to an incidence angle θ_i. The electric field directions $\vec{E}_0^{TE}$ and $\vec{E}_0^{TM}$ respectively for TE and TM polarizations are also represented in figure 1. A part of this electric field is reflected at the Air/TiO_2 interface and the rest is refracted inside the oxide layer with an angle θ_r. This refracted part is then reflected at the TiO_2/Ti interface and is again split at the TiO_2/Air interface. Multiple reflections thus occur inside the oxide layer giving rise to multiple rays emerging from the oxide layer. All rays emerging from the oxide layer have a direction θ_i relative to the sample surface perpendicular. The origin of the reflectance spectra local extrema observed for anodized titanium is the total phase-shift between two successive rays. This total phase-shift doesn't depend on the considered rays and can be for example calculated between rays I and II. As indicated in figure 1 the electric fields corresponding to rays I and II have wave-vectors denoted respectively as $\vec{k}_I$ and $\vec{k}_{II}$ and directions denoted respectively as $\vec{E}_I^{TE}$ and

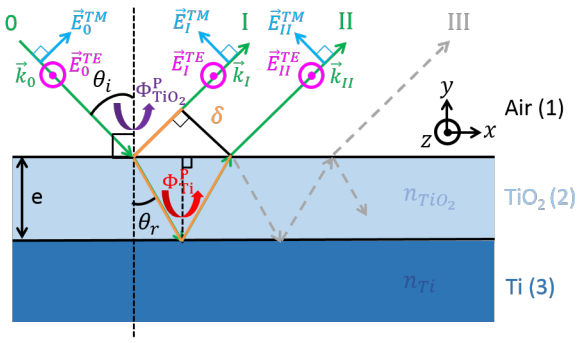

Figure 1. Description of the interference phenomenon occurring inside the oxide layer, with the various rays implied in the phenomenon and the definitions of the different parameters used in the equations: e, thickness of the oxide layer; θ_i, incidence angle; θ_r refracted angle; δ, geometrical optical path difference; $\Phi^P_{TiO_2}$, phase-shift undergone by the electric field of polarization $P = TE$ or TM at the Air/TiO_2 interface; Φ^P_{Ti}, phase-shift undergone by the electric field of polarization $P = TE$ or TM at the TiO_2/Ti interface. $\vec{E}^{TE}_j$, $\vec{E}^{TM}_j$ and $\vec{k}_j$ denote respectively the directions of the TE polarization electric field, the TM polarization electric field and the electric field wave-vector for the rays $j = 0$, I and II. The model material considered here is a perfectly flat and homogeneous layer of TiO_2 with a refractive index n_{TiO_2} on top of a semi-infinite perfectly flat and homogenous Ti substrate with a refractive index n_{Ti}. All rays emerging from the oxide layer have a direction θ_i relative to the sample surface perpendicular.

$\vec{E}^{TE}_{II}$ for TE polarization and $\vec{E}^{TM}_I$ and $\vec{E}^{TM}_{II}$ for TM polarization. Note that $\vec{k}_I = \vec{k}_{II}$ as the rays emerging from the oxide layer are all parallel to each other. Assuming monochromatic plane waves for the electric fields, the spatial variations of the different electric fields involved in the total phase-shift calculation can be written as:

$$\begin{cases} \vec{E}^P_0 = \left\|\vec{E}^P_0\right\| \vec{u}^P_0 \exp\left(i\vec{k}_0 \cdot \vec{r}\right) \\ \vec{E}^P_I = r^P_{1-2} \left\|\vec{E}^P_0\right\| \vec{u}^P_I \exp\left(i\vec{k}_I \cdot \vec{r}\right) \\ \vec{E}^P_{II} = t^P_{1-2} r^P_{2-3} t^P_{2-1} \left\|\vec{E}^P_0\right\| \vec{u}^P_{II} \exp\left(i\vec{k}_I \cdot \vec{r} + i\frac{2\pi\delta}{\lambda}\right) \end{cases}, \quad (1)$$

where $\vec{r} = x\vec{u}_x + y\vec{u}_y + z\vec{u}_z$ with $(\vec{u}_x, \vec{u}_y, \vec{u}_z)$ the orthonormal basis of the (x, y, z) coordinate system defined in figure 1. λ is the incident light wavelength. δ is the geometrical optical path difference represented in figure 1. $\|\vec{v}\|$ designates the Euclidean norm of vector $\vec{v}$. $P = TE$ or TM denotes the electric field polarization. $\vec{u}^P_j$ ($j = 0, I$ or II) are the unit vectors determining the electric field directions. r^P_{1-2}, r^P_{2-3}, t^P_{1-2} and t^P_{2-1} are the amplitude Fresnel coefficients (see chap. I of [22]) for an electromagnetic field respectively reflected at the Air/TiO_2 interface, reflected at the TiO_2/Ti interface, transmitted from Air towards TiO_2 and transmitted from TiO_2 towards Air. These coefficients depend on the incidence angle and, through n_{TiO_2} and n_{Ti}, on the wavelength λ. Note that as $\vec{k}_I = \vec{k}_{II}$ we also have $\vec{u}^P_I = \vec{u}^P_{II}$.

The total phase-shift $\Delta\varphi^P$ between rays I and II is equal to:

$$\Delta\varphi^P = \arg\left[\vec{E}^P_{II} \cdot \left(\vec{E}^P_I\right)^*\right], \quad (2)$$

where $\arg(z)$ denotes the argument of the complex number z. $\vec{u} \cdot (\vec{v})^*$ denotes the dot product between vector $\vec{u}$ and the complex conjugate of vector $\vec{v}$. If we neglect a possible imaginary part of the TiO_2 refractive index, the amplitude Fresnel coefficients t^P_{1-2} and t^P_{2-1} are positive real numbers, whereas r^P_{1-2} is a real number which sign depends on the light polarization and on the light incidence angle. In this case, when developing the expression of the geometrical optical path difference δ, $\Delta\varphi^P$ can be written as:

$$\Delta\varphi^P = \frac{4\pi e n_{TiO_2} \cos(\theta_r)}{\lambda} + \Phi^P \quad (3)$$

where Φ^P corresponds to the interfaces phase-shift for polarized light. e is the thickness of the oxide layer. We have:

$$\Phi^P = \Phi^P_{Ti} - \Phi^P_{TiO_2} \quad \text{with} \quad \begin{cases} \Phi^P_{TiO_2} = \arg\left(r^P_{1-2}\right) \\ \Phi^P_{Ti} = \arg\left(r^P_{2-3}\right) \end{cases}, \quad (4)$$

where $\Phi^P_{TiO_2}$ and Φ^P_{Ti} are the phase-shifts undergone by the electric field of polarization $P = TE$ or TM when reflected respectively at the Air/TiO_2 interface and at the TiO_2/Ti interface. Note that we have the relationship $\cos(\theta_r) = \sqrt{1 - \left(\frac{\sin(\theta_i)}{n_{TiO_2}}\right)^2}$. n_{TiO_2} depends on the wavelength λ, and so does θ_r. As we neglect a possible imaginary part for n_{TiO_2}, $\Phi^P_{TiO_2}$ is equal to 0 or π, depending on the light polarization and on the light incidence angle.

For a local maximum of the reflectance spectrum, we have a constructive interference. For a local minimum, we have a destructive interference. We thus have (see chap. VII of [22]):

$$\begin{cases} \text{for a maximum: } \Delta\varphi^P = 2m^P\pi, \quad m^P \in \mathbb{N}^* \\ \text{for a minimum: } \Delta\varphi^P = 2m^P\pi, \quad m^P \in \mathbb{N} + \frac{1}{2} \end{cases}, \quad (5)$$

for $P = TE$ or TM. We can thus deduce from the minima and maxima positions the value of the oxide thickness, if the TiO_2 and Ti refractive indexes are known at the corresponding wavelengths:

$$\begin{cases} \text{for a position } \lambda_{max} \text{ of a maximum:} \\ e = \frac{\lambda_{max}}{4\pi n_{TiO_2}\cos(\theta_r)} \times \left[2m^P\pi - \Phi^P\right], \quad m^P \in \mathbb{N}^* \\ \text{for a position } \lambda_{min} \text{ of a minimum:} \\ e = \frac{\lambda_{min}}{4\pi n_{TiO_2}\cos(\theta_r)} \times \left[2m^P\pi - \Phi^P\right], \quad m^P \in \mathbb{N} + \frac{1}{2} \end{cases} \quad (6)$$

for $P = TE$ or TM.

In the following, three different cases will be considered: TE polarized light, TM polarized light and non-polarized light. For non-polarized light,

the thickness value is obtained as an average of the thickness values obtained for TE and TM polarization. For non-polarized light, the oxide thickness is thus computed through the following formulas:

$$\begin{cases} \text{for a position } \lambda_{max} \text{ of a maximum:} \\ e = \dfrac{\lambda_{max}}{4\pi n_{TiO_2}\cos(\theta_r)}\left[(m^{TE}+m^{TM})\pi - \dfrac{\Phi^{TE}+\Phi^{TM}}{2}\right] \\ \left(m^{TE}, m^{TM}\right) \in \mathbb{N}^{*2}, \\ \text{for a position } \lambda_{min} \text{ of a minimum:} \\ e = \dfrac{\lambda_{min}}{4\pi n_{TiO_2}\cos(\theta_r)}\left[(m^{TE}+m^{TM})\pi - \dfrac{\Phi^{TE}+\Phi^{TM}}{2}\right] \\ \left(m^{TE}, m^{TM}\right) \in \left(\mathbb{N}+\dfrac{1}{2}\right)^2. \end{cases} \quad (7)$$

Note that the interference orders m^{TE} and m^{TM} aren't necessary the same. It will be shown in the following that in some cases, a given extremum position can be a minimum for TE polarized light and a maximum for TM polarized light, and vice versa.

When the interfaces phase-shift isn't taken into account, the formulas giving the oxide thickness from the reflectance spectra local extrema don't depend on the light polarization and become:

$$\begin{cases} \text{for a position } \lambda_{max} \text{ of a maximum:} \\ e = \dfrac{\lambda_{max}}{4\pi n_{TiO_2}\cos(\theta_r)} \times 2m\pi \quad m \in \mathbb{N}^* \\ \text{for a position } \lambda_{min} \text{ of a minimum:} \\ e = \dfrac{\lambda_{min}}{4\pi n_{TiO_2}\cos(\theta_r)} \times 2m\pi \quad m \in \mathbb{N}+\dfrac{1}{2} \end{cases}. \quad (8)$$

3. Samples preparation and characterization

3.1. Samples preparation

In section 2, an anodized titanium sample has been modeled as a homogeneous oxide layer above a semi-infinite titanium substrate. All interfaces are supposed to be perfectly flat. To check if the theoretical observations are valid for experimental samples, two anodized titanium samples have been prepared with two different roughness values.

The samples were cut out from a 1 mm thick ASTM Grade 2 titanium sheet. A simple polishing with a SiC P300 grinding paper was first performed. Then, a complete mechanical polishing has been carried out, including diamond paste solutions from 6 µm to 1 µm and a final step using a grinding cloth and an alumina solution with a particle size of 0.6 µm. The first sample referred to as 'Alumina' isn't further polished. The second sample referred to as 'Vibromet' is then submitted to a vibratory polisher, Buehler Vibromet2, with a 60 mm colloidal solution. The samples were anodized in a galvanostatic regime by imposing a current density equal to 20 mA cm^{-2}. The counter electrode is circular and made of activated titanium. All experiments were performed in a 0.5 M sulfuric acid electrolytic solution (H_2SO_4) at room temperature. The cell potential increases gradually during the anodizing process. When the potential reaches 90 V, the current is shut down and the sample is removed from the bath. Figure 2 is a picture of the two samples. The samples are colored because of the interference phenomenon occuring inside the oxide layer. The typical order of magnitude of the oxide layer thickness for titanium anodized in similar conditions is in about 170 nm to 200 nm [2, 23], explaining the pink color of the samples.

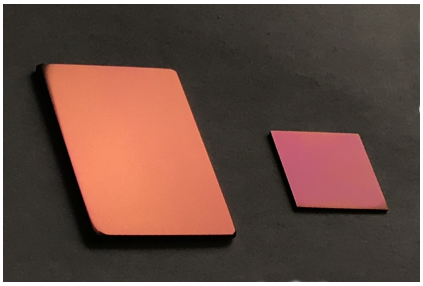

Figure 2. Picture of the Vibromet (left) and Alumina (right) samples. The picture has been taken under diffuse halogen light, with a camera having an automatic white balance.

3.2. Samples roughness characterizations

Roughness measurements have been carried out by a non-contact white light interferometric optical system, Bruker Nanoscope Wyko® NT9100, before anodizing to obtain the roughness of the titanium substrate, and after anodizing for the roughness of the oxide layer. The size of the measured area is 1.15 mm× 0.86 mm. For each sample, nine roughness measurements have been made. Table 1 presents the S_a roughness parameter [24] for the samples before and after anodizing. The values correspond to the average over the nine measurements with uncertainties equal to the standard deviation over these measurements. The anodizing process clearly modifies the sample roughness, with a S_a paramter increased by a factor of about 3 for the Vibromet sample and by a factor of about 2 for the Alumina sample.

Table 1. Samples S_a roughness parameters before and after anodizing. The values correspond to the average over nine measurements with uncertainties equal to the standard deviation over these measurements.

Sample name	Roughness before anodizing	Roughness after anodizing
Vibromet	15 ± 1 nm	48 ± 1 nm
Alumina	59 ± 2 nm	130 ± 6 nm

3.3. Samples reflectance measurements

The reflectance measurements have been performed with an in-plane goniometer (see figure 3). The goniometer source is a Laser Driven Light Source connected with a 100 µm core diameter optical fiber to an arm equipped with a lens with a 50 mm focal length, a polarizer and a 10 mm×2 mm slit. The beam incident on the sample is collimated. The detection arm is equipped with a 2 inches diameter integrating sphere connected with a 1 mm core diameter optical fiber to a CCD array spectrometer. The integrating sphere is placed 7 cm far from the sample surface and has an aperture of 0.5 inches. The goniometer is used in a specular configuration, with the detection angle and the incidence angle both equal to θ_i.

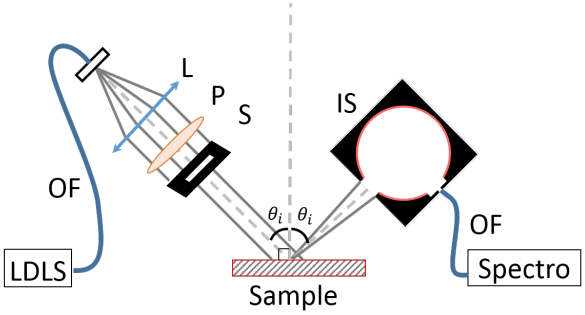

Figure 3. Optical layout of the goniometer used for the reflectance mesurements. The goniometer source is a Laser Driven Light Source (LDLS) connected with a 100 µm core diameter optical fiber (OF) to an arm equipped with a lens (L) with a 50 mm focal length, a polarizer (P) and a 10 mm×2 mm slit (S). The beam incident on the sample is collimated. The detection arm is equipped with a 2 inches diameter integrating sphere (IS) connected with a 1 mm core diameter optical fiber (OF) to a CCD array spectrometer (spectro). The integrating sphere is placed 7 cm far from the sample surface and has an aperture of 0.5 inches. The goniometer is used in a specular configuration, with the detection angle and the incidence angle both equal to θ_i.

4. Results and discussion

4.1. Theoretical estimation of the accuracy of the oxide thickness determination from the local extrema positions

The formulas presented in section 2 have been applied to simulated reflectance spectra with known oxide thicknesses. The oxide thickness values extracted from the local extrema positions have been compared to the oxide thickness values put as parameters of the simulations in order to estimate the accuracy of the formulas. The reflectance spectra have been simulated in the wavelength range [370 nm 800 nm] by using an Abeles matrices formalism [25]. The model material considered here is the same as on figure 1. The titanium and oxide layer refractive indexes used in the simulations are the followings (see figure 4): the titanium refractive index is extracted from [26] and the oxide layer refractive index is the refractive index measured in [20] for the "quasi-amorphous" oxide layer obtained in the case of titanium anodized in a 1 N sulfuric acid electrolyte.

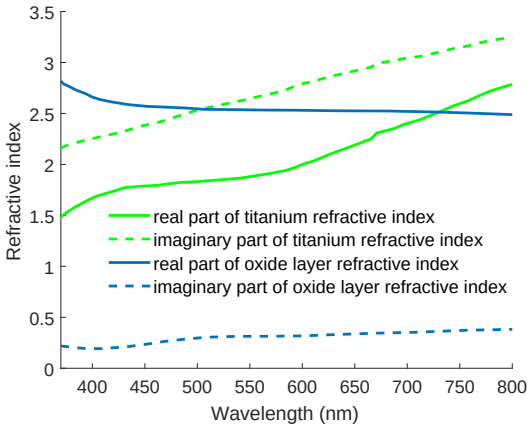

Figure 4. Titanium and oxide layer refractive indexes used in the reflectance spectra simulations. The titanium refractive index is extracted from [26] and the oxide layer refractive index is the refractive index measured in [20] for the "quasi-amorphous" oxide layer obtained in the case of titanium anodized in a 1 N sulfuric acid electrolyte.

The oxide layer thickness of anodized titanium is usually comprised from about ten to a few hundreds nanometers [1, 2, 10, 13]. The reflectance spectra have thus been computed for oxide thicknesses from 20 nm to 200 nm. The reflectance spectra have been also computed for different incidence angles from 0° to 80° and for TE, TM and non-polarized light. The non-polarized reflectance spectrum is obtained as an average of the TE and TM reflectance spectra. All local extrema positions for all simulated spectra have been extracted (see figure 5).

The number of local extrema depends on the oxide thickness. It generally goes (in the wavelength range [370 nm 800 nm]) from 1 for a 20 nm thick oxide layer to 4 for a 200 nm thick oxide layer. For incidence angles above 70°, shifts of the local extrema positions are observed for TM and non-polarized light, with sometimes modifications of the extrema numbers. For example, for TM polarized light and an oxide thickness of 180 nm, the reflectance spectra exhibit 3 local extrema for all incidence angles besides 70° where it exhibits 4 local extrema. Also, for non-polarized light and an oxide thickness of 140 nm, the reflectance spectra exhibit 3 local extrema for incidence angles from 0° to 70° and 5 local extrema for an incidence angle of 80°.

Then the oxide thicknesses have been computed,

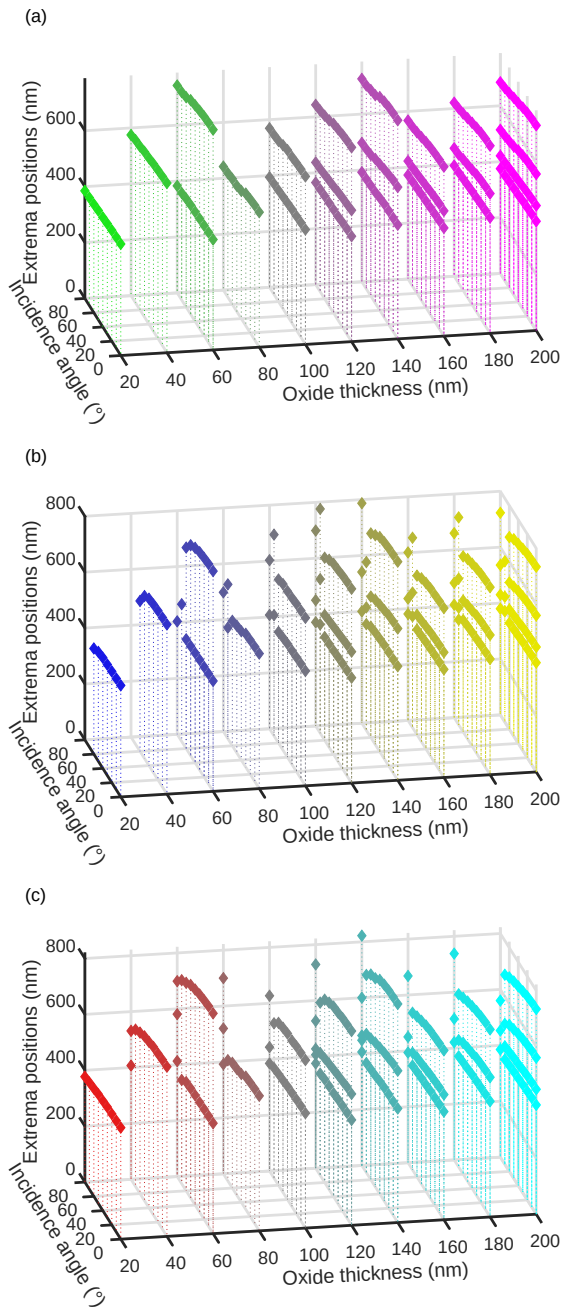

Figure 5. Extrema positions of the various reflectance spectra of anodized titanium computed in the wavelength range [370 nm 800 nm] for incidence angles between 0° and 80° and oxide thicknesses between 20 nm and 200 nm for (*a*) TE, (*b*) TM and (*c*) non-polarized light. Note that for TM polarized light, for oxide thicknesses below 60 nm, the reflectance spectra don't exhibit local extrema for incidence angles higher than 60°.

first with taking into account the interfaces phase-shift through equations 6, 7 and then, when neglecting the phase-shift though equation 8. Figure 6 represents the different interference orders used to compute the oxide thickness when the phase-shift is taken into account, for TE, TM and non-polarized light. For a minimum, the interference order is a half-integer. For a maximum, the interference is an integer. The interference orders increase with the oxide thickness, starting with a value of 0.5 for a 20 nm thick oxide layer, up to 3 or 3.5 for a 200 nm thick oxide layer. For TM polarized light (as well as for m_{TM} for non-polarized light) and for incidence angles above 70° a jump of 0.5 is observed in the interference orders. When looking at the reflectance spectra, this jump corresponds to switches from a mininum to a maximum (or vice versa) for a same extremum position. This phenomenon is due to an additional π phase-shift which occurs at the reflection on the air/oxide interface for incidence angles above about 70° : this will be detailed and discussed later. When the phase-shift is neglected (equation 8) the interference orders are the same as previously for TE polarized light. For TM polarized light, the interference orders are the same for incidence angles below 70°. For incidence angles above 70°, the interference orders are lowered by 0.5, as the additional air/oxide interface π phase-shift is not taken into account. For non-polarized light, the interference orders correspond to m_{TE}.

The relative error E on the oxide thickness as been computed, through the following formula:

$$E(\%) = 100 \times \frac{|e_{eval} - e_{simu}|}{e_{simu}}, \tag{9}$$

where e_{eval} is the oxide thickness evaluated from the reflectance spectra local extrema and e_{simu} is the oxide thickness value put in the reflectance spectra simulations. When the reflectance spectra exhibit more than one local extremum, e_{eval} is an average over the oxide thickness values obtained from all local extrema positions. Figure 7 represents the relative error E on the oxide thickness as a function of the oxide thickness and the light incidence angle for TE, TM and non-polarized light, when the phase-shift is taken into account and when it is neglected. When the phase-shift is neglected, for all polarization states, a global decrease of the relative error with the oxide thickness is observed. This is due to the fact that the error made when neglecting the interfaces phase-shift doesn't depend on the interference order. When comparing equations 6 and 8 or equations 7 and 8, the corrections terms linked to the interfaces phase-shift are either $-\lambda_{ext}\Phi^P / (4\pi n_{TiO_2} \cos\theta_r)$ or $-\lambda_{ext} \left(\Phi^{TE} + \Phi^{TM}\right) / (8\pi n_{TiO_2} \cos\theta_r)$ with λ_{ext} the local extremum position, which don't depend on the interference order. As observed on figure 6, the extrema orders increase with the oxide thickness, explaining the decrease of the relative error with the oxide thickness. For TE polarized light, the incidence angle doesn't have a significant influence on the relative error. For non-polarized light, and particularly for TM polarized light, an increase of

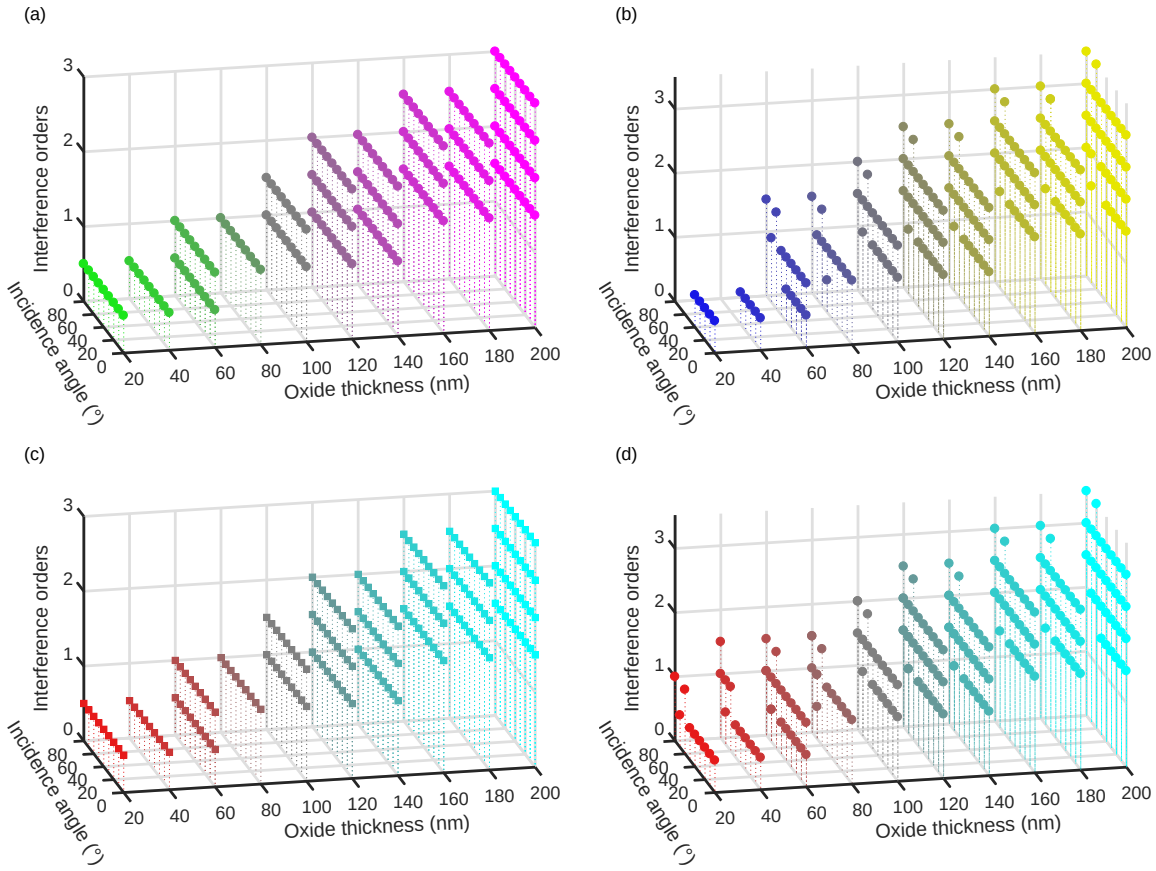

Figure 6. Interference orders corresponding to the local extrema positions presented in figure 5 and used to compute the oxide thickness when taking into account the electromagnetic phase-shift (equations 6 and 7) for (*a*) TE, (*b*) TM and (*c*),(*d*) non-polarized light. (*c*) corresponds to the interference order m_{TE} of equation 7 and (*d*) to m_{TM}.

the relative error is observed at incidence angles higher than 70°. Neglecting the interfaces phase-shift isn't adapted to characterize samples with thin oxide thicknesses (the relative error is higher than 85 % for a 20 nm thick oxide layer for all polarization states). Note that the smallest relative error is still of about 9 %, obtained in the case of a 200 nm thick oxide layer for all polarization states and incidence angles below 70°. When the phase-shift is taken into account, the parameter which has the main influence on the relative error is the incidence angle. The smallest relative error variations are observed for TE polarized light. For TE polarized light, the highest relative errors are obtained for oxide thicknesses between 40 nm and 80 nm, with a highest value of about 10 %. For other oxide thickness values, the relative error lies between less than 1 % to about 3 %. The highest relative error variations are observed for TM polarized light. The relative error is particularly high for an incidence angle of 70°, reaching about 43 % for an oxide thickness of 80 nm. Note that for an incidence angle of 80°, the relative error is very lower than for 70°, with relative error values lying between 1 % and 3 %. The smallest relative error values lie in the area defined by the oxide thickness range [100 nm 200 nm] and the incidence angle range [0° 60°], with variations between 1 % and 5 %. For non-polarized light, the relative error is particularly high for an incidence angle of 80°, with a maximum value of 21 % for an oxide thickness of 40 nm. The smallest relative error values lie in the area defined by the oxide thickness range [100 nm 200 nm] and the incidence angle range [0° 70°], with variations between 1 % and 6 %. Taking into account the interfaces phase-shift to compute the oxide thickness from the reflectance spectra local extrema positions thus greatly improves the oxide thickness estimation accuracy, particularly for thin oxide layers. The best results are obtained in the case of TE polarized light for all incidence angles, whereas for TM and non-polarized light, high oxide thickness estimation errors are observed for incidence angles of respectively 70° and 80°.

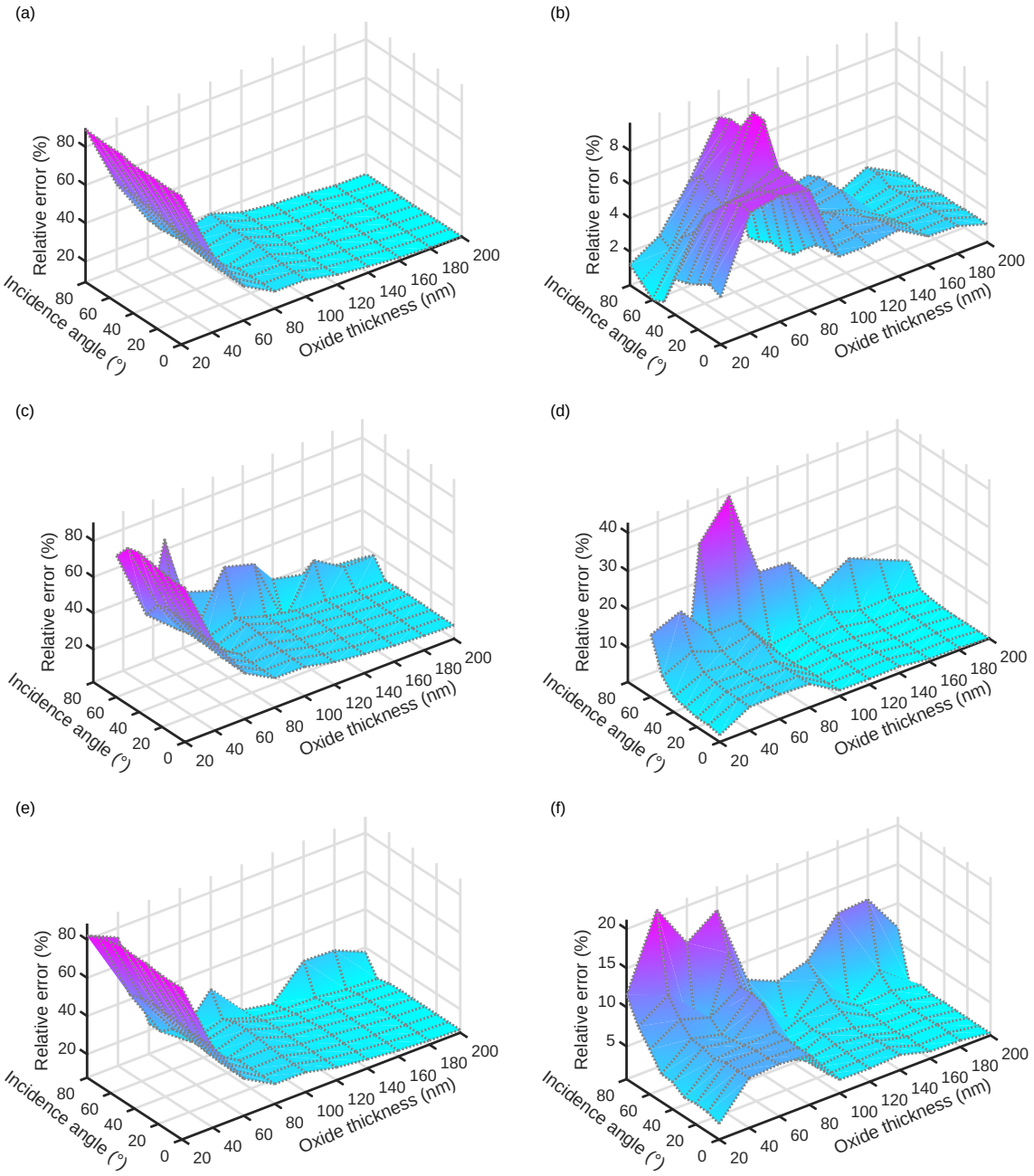

Figure 7. Relative error E on the oxide thickness computed through equation 9 as a function of the oxide thickness and the light incidence angle: (a), (c) and (e) when the interfaces phase-shift is neglected, (b), (d) and (f) when the interfaces phase-shift is taken into account; (a) and (b) for TE polarized light, (c) and (d) for TM polarized light, (e) and (f) for non-polarized light.

4.2. Correlation between oxide thickness determination accuracy and discrepancy between oxide thickness values from different extrema when the phase-shift is taken into account

As observed on figure 5, for oxide thicknesses higher than 60 nm, the reflectance spectra exhibit generally several local extrema in the wavelength range [370 nm 800 nm]. The discrepancy between the oxide thickness values obtained from the different extrema has been studied by computing the relative bias corrected standard deviation σ_R, defined with the following formula:

$$\sigma_R(\%) = 100 \times \frac{\sqrt{\sum_{i=1}^{n_o} (e_i - \bar{e})^2}}{\bar{e}\sqrt{n_o - 1}}, \tag{10}$$

where n_o is the number of extrema of the considered reflectance spectrum, e_i is the oxide thickness obtained from the extrema numbered i and $\bar{e}$ is the average oxide

thickness over all the local extrema of the considered reflectance spectrum. When the reflectance spectrum has only one extremum, we have $\sigma_R = 0$. Figure 8 represents σ_R as a function of the oxide thickness and the light incidence angle for TE, TM and non-polarized light, when the phase-shift is taken into account. As

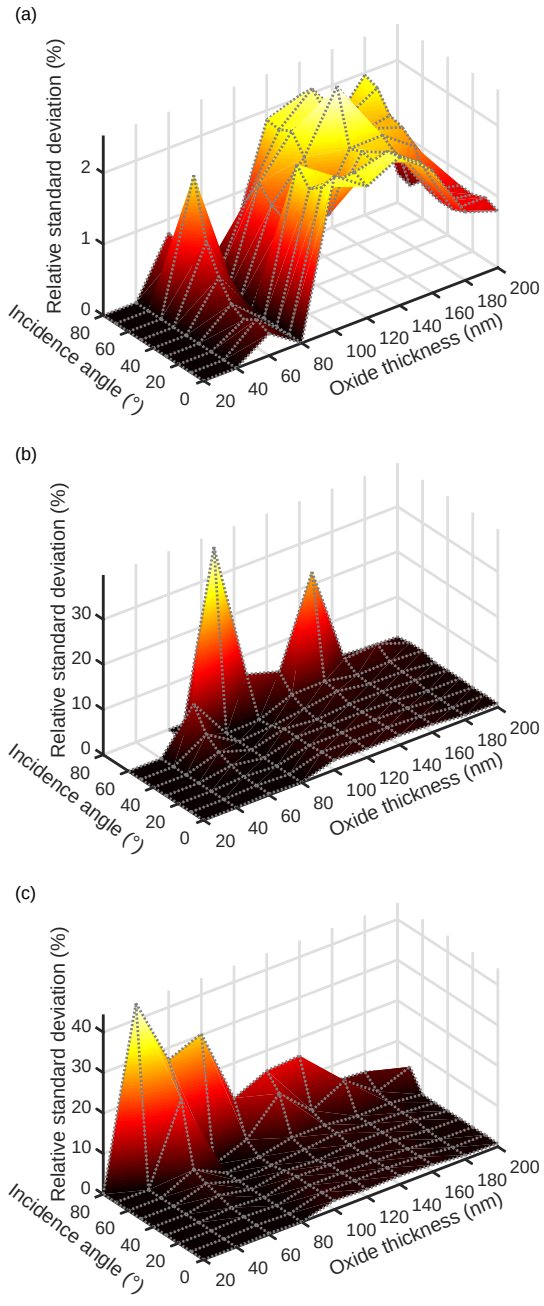

Figure 8. Relative standard deviation σ_R over the different oxide thickness values obtained from the different local extrema of a reflectance spectrum computed through equation 10 for (*a*) TE, (*b*) TM and (*c*) non-polarized light. When the reflectance spectrum exhibits one local extremum $\sigma_R = 0$.

for the relative error E, the smallest variations of σ_R are observed for TE polarized light. Also, for TM and non-polarized light, the highest values of σ_R are observed respectively for incidence angles of 70° and 80°. The correlation coefficient between E and σ_R, calculated by regrouping all polarization states and by omitting the cases where the reflectance spectra have only one extremum, is 0.7. Knowing σ_R gives thus a relatively good estimation of the relative error on the oxide thickness. σ_R and E are linked by a regression coefficient of about 0.9: $\sigma_R \simeq 0.9E$.

4.3. Origin of the high error on the oxide thickness determination for TM and non-polarized light at high incidence angles

As observed on figure 7, even when the interfaces phase-shift is taken into account, high values of the relative error E and the relative standard deviation σ_R are observed for TM and non-polarized light, for incidence angles above 70°. To understand the origin of this phenomenon, E and σ_R have been represented for incidence angles between 10° and 80°, with additional points between 60° and 80° for an oxide thickness of 160 nm, for TE, TM and non-polarized light (see figure 9). The behavior of E and σ_R starts clearly to depend

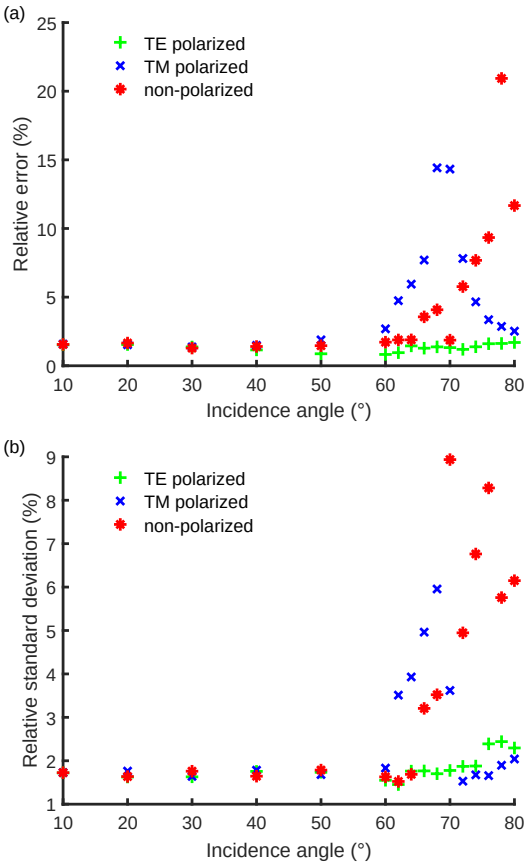

Figure 9. (*a*) Relative error E and (*b*) relative standard deviation σ_R for an oxide thickness of 160 nm for incidence angles between 10° and 80° for TE, TM and non-polarized light.

on the polarization for incidence angles above 60°. The lowest variations with the incidence angle as well as the lowest values of E are observed for TE polarized light. For TM polarized light, E exhibits a peak centered at about 69°, whereas for non-polarized light, a global increase of E with the incidence angle is observed above an incidence angle of about 65°. For σ_R, almost the same observations can be made, despite some slight differences. For TE polarized light, σ_R exhibits slightly higher values than for TM polarized light at incidence angles above 72°. For TM polarized light, σ_R doesn't exhibit a peak as well marked as for E, but its highest values are observed around the same incidence angles as for E. Also, for non-polarized light, the increase of σ_R with the incidence angle is more "noisy".

Figure 10 represents the reflectance spectra in the case of an oxide thickness of 160 nm for incidence angles between 60° and 80° for TE, TM and non-polarized light. For TE polarized light, the reflectance spectra keep the same shape for all incidence angles. For TM polarized light, a shift of the local extrema positions is observed, leading progressively to a switch from a position corresponding to a minimum to a position corresponding to a maximum (or vice-versa). This phenomenon is due to an additional π phase-shift which occurs at the reflection on the air/oxide interface for incidence angles above the Brewster angle of the air/oxide interface. The Brewster angle corresponds to a cancellation of the TM polarized light Fresnel reflectance coefficient of the air/oxide interface (denoted r_{1-2}^{TM} in section 2). As the TiO_2 refractive index is wavelength depend, the Brewster angle will also be wavelength depend. As observed on figure 11, for the TiO_2 refractive index considered in the present paper, in the wavelength range [370 nm 800 nm], the air/TiO_2 interface Brewster angle is between 68.5° and 70.5°, decreasing with the wavelength. Close to the Brewster angle, the TM polarized light reflectance spectra local extrema positions are thus highly shifted from the theoretical positions predicted by assuming constructive or destructive interferences (equation 6). This explains the high values of E and σ_R observed for TM polarized light around an incidence angle of 69° (see figure 9). For non-polarized light, a modification of the shape of the reflectance spectra is also observed when the incidence angle goes from 60° to 80°, with shifts of the local extrema positions. As non-polarized light reflectance spectra are averages of TE and TM polarized light reflectance spectra, when an extremum position corresponds to a mimimum for TE polarized light and a maximum for TM polarized light (or vice-versa), the extremum positions are totally shifted from the theoretical prediction of equation 7. This is the case for incidence angles above the air/TiO_2 interface Brewster angle, which explains the increase of E and σ_R for incidence angles above 65° (see figure 9).

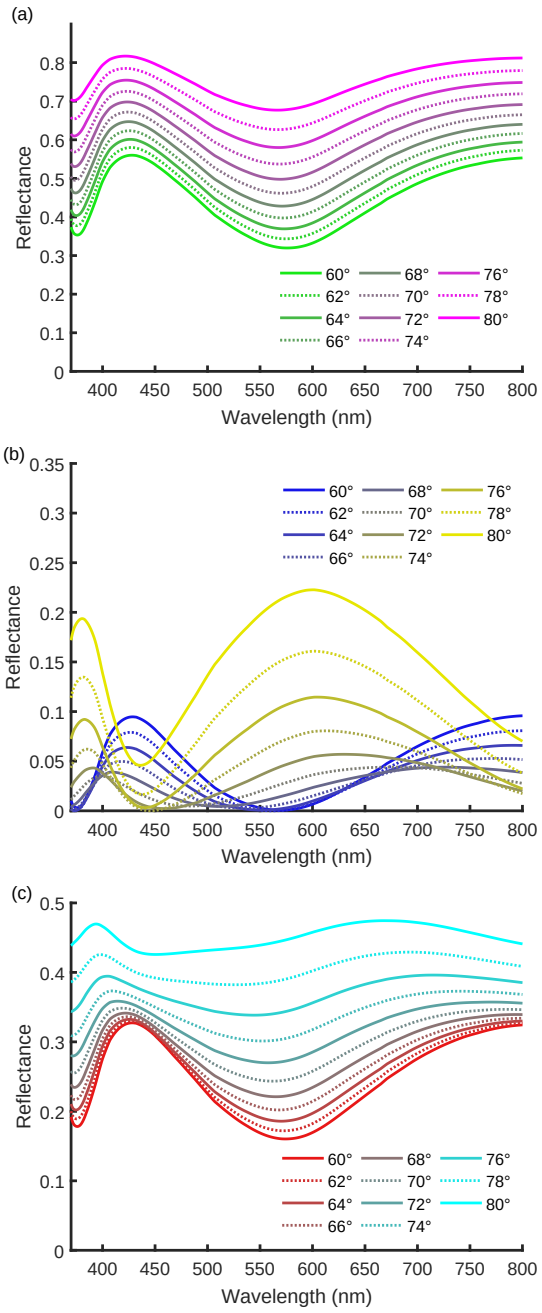

Figure 10. Simulated reflectance spectra in the case of an oxide thickness of 160 nm for incidence angles between 60° and 80° for (*a*) TE, (*b*) TM and (*c*) non-polarized light.

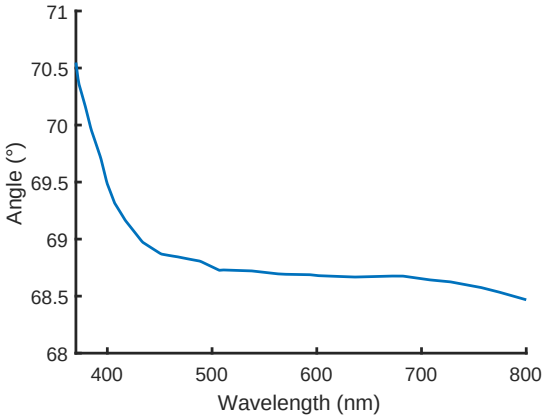

Figure 11. Brewster angle vs wavelength for the air/TiO_2 interface computed from the TiO_2 refractive index presented in figure 4.

4.4. Application to anodized titanium samples

To check if the theoretical results presented previously are valid for experimental samples, the TE, TM and non-polarized reflectance spectra of the Alumina and Vibromet samples (see figure 2) have been measured with the in-plane goniometer described in figure 3. The reflectance spectra have been measured for incidence angles between 15° and 80° in the wavelength range [370 nm 800 nm]. Figure 12 presents the experimental reflectance spectra for the Alumina sample for TE, TM and non-polarized light, for incidence angles between 60° and 80°, that is close to the air/TiO_2 interface Brewster angle. The experimental spectra exhibit a similar behavior as the simulated ones (see figure 10). For TE polarized light, the reflectance spectra keep the same shape for all incidence angles. For TM polarized light, a shift of the local extrema positions is observed, leading progressively to a switch from a position corresponding to a minimum to a position corresponding to a maximum (and vice-versa). For non-polarized light, a modification of the shape of the reflectance spectra is observed, accompanied by a shift of the local extrema positions.

The extrema of these experimental spectra have been extracted the same way as for the simulated ones. Then, according to equations 7 and 6 taking into account the phase-shift, the oxide layer thickness has been computed for all extrema. The titanium and oxide layer refractive indexes used to compute the oxide layer thickness are the same as for the simulated spectra. Note that the refractive indexes of the samples are certainly different from these values, and this will induce a bias on the absolute value of the oxide layer thickness. The purpose here is not to obtain the absolute value of the oxide layer thickness, but to check if the observations made on the simulated spectra,

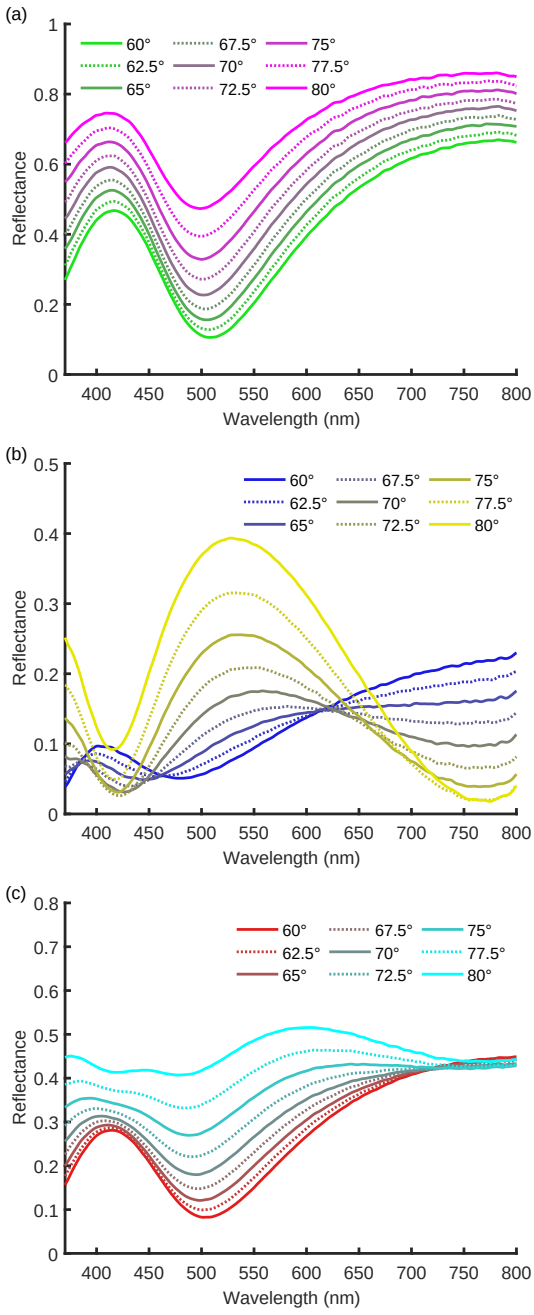

Figure 12. Measured reflectance spectra of the Alumina sample for incidence angles between 60° and 80° for (*a*) TE, (*b*) TM and (*c*) non-polarized light. These spectra have been obtained by smoothing the raw experimental spectra by a gaussian filter with a 10 nm window.

which are based on the simple model material of figure 1, are still valid for anodized titanium samples. Key features of these observations are the variations of the relative standard deviation σ_R with the incidence angle and the polarization (see figures 8 and 9(*b*)). σ_R has thus been computed from the experimental spectra for the Alumina and the Vibromet samples. To reduce the influence of the measurement noise on σ_R, the

raw experimental spectra have been smoothed by a gaussian filter with a 10 nm window. The results are presented in figure 13.

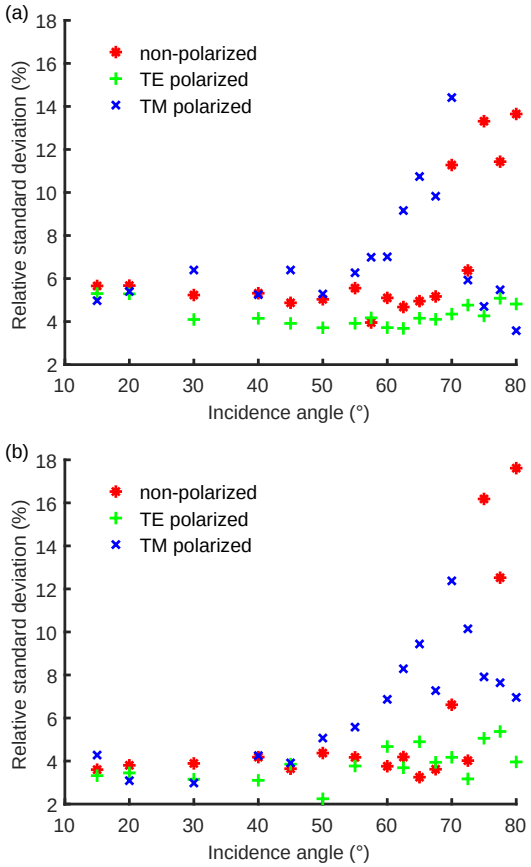

Figure 13. Relative standard deviation σ_R for (a) the Alumina sample and (b) the Vibromet sample for incidence angles between 15° and 80° for TE, TM and non-polarized light.

The variations of σ_R with the incidence angle exhibit similar shapes for both samples, with similar values. These values are basically twice higher than the simulated values of figure 9(b). Experimental and simulated data both have similar variations with the incidence angle, despite a more noisy behavior for experimental data. For incidence angles below 60°, σ_R has similar values for all polarizations. Whereas σ_R keeps low values for TE polarized light for incidence angles above 60°, σ_R exhibit a peak for TM polarized light at 70°. For non-polarized light, σ_R starts to increase for incidence angles higher than about 70°. The similar behavior of σ_R with the incidence angle for both experimental and simulated data confirms that the conclusions deduced from the simulated data are suitable for anodized titanium samples. It can be noted that despite the S_a roughness parameter of the Alumina sample after anodizing is the same order of magnitude as its oxide layer thickness, the model used here, which assumes perfectly flat interfaces (see figure 1), correctly predicts the behavior of σ_R for this sample.

5. Conclusion

The present paper concerns the oxide layer thickness determination of oxidized metals in the case where an optical interference phenomenon occurs inside the oxide layer. The paper focuses on anodized titanium. It establishes theoretical formula to compute the oxide layer thickness from the local extrema positions of the material reflectance spectra. These formula take into account the electromagnetic phase-shift with occurs at the reflection on the air/oxide and oxide/metal interfaces and are valid for TE, TM and non-polarized light, and for all incidence angles. By applying these formula to simulated reflectance spectra with known oxide thicknesses, it shows that neglecting the interfaces phase-shift is inappropriate to determine the oxide thickness of samples with thin oxide thicknesses : the relative error is higher than about 30 % for oxide thicknesses thinner than 60 nm. When the interfaces phase-shift is taken into account, a careful attention needs to be paid to the light polarization for incidence angles close to the Brewster angle of the air/oxide interface (typically for incidence angles higher than 60° for the case studied here). Whereas the relative error on the oxide thickness is always below 10 % for TE polarized light, it can reach 40 % for TM polarized light (incidence angle of 70° and oxide thickness of 80 nm) and 20 % for non-polarized light (incidence angle of 80° and oxide thickness of 40 nm). The relative error is relatively good correlated to the relative standard deviation characterizing the discrepancy of the oxide thickness values obtained from different extrema positions. This relative standard deviation has been computed for anodized titanium samples. The behavior of the relative standard deviation with polarization and incidence angle is similar to the behavior predicted from the simulation, confirming that the theoretical study is suitable for anodized titanium.

Acknowledgments

This work was partly supported by the LABEX MANUTECH-SISE (ANR-10-LABX-0075) of Université de Lyon, within the program "Investissements d'Avenir" (ANR-11-IDEX-0007) operated by the French National Research Agency (ANR).
The collaboration between Mines Saint-Etienne and Politecnico di Milano on this study was partly funded by the CMIRA program for international collaborations of Region Auvergne Rhone-Alpes.

References

[1] Van Gils S, Mast P, Stijns E and Terryn H 2004 *Surface and Coatings Technology* **185** 303–310 ISSN 02578972

[2] Diamanti M V, Del Curto B and Pedeferri M 2008 *Color Research & Application* **33** 221–228 ISSN 03612317

[3] Gallant D, Pézolet M and Simard S 2006 *Journal of Physical Chemistry B* **110** 6871–6880 ISSN 15206106

[4] Wosu S N 2007 *Journal of Materials Science* **42** 4087–4097 ISSN 00222461

[5] Jerkiewicz G, Zhao B, Hrapovic S and Luan B L 2008 *Chemistry of Materials* **20** 1877–1880 ISSN 08974756

[6] Sheng C C, Cai Y Y, Dai E M and Liang C H 2012 *Chinese Physics B* **21** ISSN 16741056

[7] Komatsu I, Aoki H, Ebisawa M, Kuroda A, Kuroda K and Maeda S 2016 *Thin Solid Films* **603** 180–186 ISSN 00406090

[8] Bartlett L 2009 *Variability in coloured titanium surfaces for jewellery* Ph.D. thesis University of the Arts London

[9] Di Quarto F, Doblhofer K and Gerischer H 1978 *Electrochimica Acta* **23** 195

[10] Sharma A K 1992 *Thin Solid Films* **208** 48–54 ISSN 00406090

[11] Karambakhsh A, Afshar A, Ghahramani S and Malekinejad P 2011 *Journal of Materials Engineering and Performance* **20** 1690–1696 ISSN 1059-9495

[12] Manjaiah M and Laubscher R F 2017 *Surface and Coatings Technology* **310** 263–272 ISSN 02578972

[13] Balaji U and Pradhan S K 2018 *Materials and Design* **139** 409–418 ISSN 18734197

[14] Yang C l, Chen F l and Chen S w 2006 *Materials Chemistry and Physics* **100** 268–274 ISSN 02540584

[15] Diamanti M, Spreafico F and Pedeferri M 2013 *Physics Procedia* **40** 30–37 ISSN 18753892

[16] Fuhrman F G and Collins F C 1977 *J. Electrochem. Soc.* 1294–1299 ISSN 00134651

[17] Charlesby A and Polling J 1954 *Proceedings of the Royal Society of London A* **227** 434–447 ISSN 1364-5021

[18] Winterbottom A B 1946 *Transactions of the Faraday Society* **42** 487–495 ISSN 00147672

[19] Pliskin W A 1968 *Solid State Electronics* **11** 957–963 ISSN 00381101

[20] Blondeau G, Froelicher M, Froment M and Hugot-Le Goff A 1977 *Thin Solid Films* **42** 147–153 ISSN 00406090

[21] Joseph J and Gagnaire A 1983 *Thin Solid Films* **103** 257–265 ISSN 00406090

[22] Born M and Wolf E 1980 *Principles of optics : electromagnetic theory of propagation, interference and diffraction of light* (Pergamon Press) ISBN 9780080264820

[23] Cridling Q, Charriere R, Jamon D, Diamanti M V, Pedeferri M P and Delafosse D 2017 *IS&T International Symposium on Electronic Imaging 2017 - Material Appearance 2017* 86–91 ISSN 24701173

[24] Whitehouse D 2002 *Surfaces and Their Measurement* (Elsevier) ISBN 9781903996010

[25] Abelès F 1950 *Le Journal de Physique et le Radium* **11** 307–309

[26] Lynch D W, Olson C G and Weaver J H 1975 *Physical Review B* **11** 3617